Advanced Engineering Science
http://publish.mersin.edu.tr/index.php/ades
e-ISSN 2791-8580

The effect of molding and gating system design on hydrogen induced crack defects in steel castings

Mustafa Murat Zor*[1], Ferhat Tülüce[1], Serdar Kesim[1], Alper Yoloğlu[1]

[1]*ÇİMSATAŞ Çukurova Construction Machinery IND. TRADE. A.S. Mersin, Türkiye, foundry@cimsatas.com*

Cite this study: Zor, M. M., Tülüce, F., Kesim, S. & Yoloğlu, A. (2023). The effect of molding and gating system design on hydrogen induced crack defects in steel castings. Advanced Engineering Science, 3, 164-177

Keywords
Hydrogen induced cracking
Steel casting
Gating system design
Molding design
Modelling and simulation

Research Article
Received:11.09.2023
Revised: 19.10.2023
Accepted: 27.10.2023
Published:30.10.2023

Abstract

Hydrogen cracking occurs due to the build-up of gas pressure at inclusions, generally manganese sulfide inclusions. Cracking occurs in the thickest parts of a section, distance to diffuse out to surface is greater, and hydrogen is more likely to get trapped. Casting simulation technology is an most effective method to provide the predicted information on casting defects such as shrinkage, gas entrapment, and non-metallic inclusions. But it is not possible to detect hydrogen-induced defects in steel castings in today's flow and solidification simulation programs. In the study, various moulding and gating system designs have been designed for steel castings in industrial conditions and the effects of gating system design on hydrogen-induced crack defects have been investigated. The flow and solidification of the gating systems of the casting part were simulated by using Novacast flow and solidification program. The study clearly shows that gating system has revealed that it plays a significant role in preventing hydrogen-induced crack defects in steel castings.

1. Introduction

It is well known to foundry that hydrogen in steels can cause cracks termed as hairline, shatter or flakes, especially in low alloy NiCr, NiCrMo, NiCrMoV types their prevalence in ingots, as opposed to steel castings appears -to arise from massive cross section thicknesses (rather more than module 4 cm) promoting hydrogen retention for cracking and embrittlement events. Nevertheless, effective and economic means for hydrogen control should be considered especially in large section low-alloy steel castings. Hydrogen has been and always will be a source of various problems within steel production because of its generally detrimental effects on processing characteristics and service performance of steel casting parts. If the hydrogen content of the molten steel exceeds the solubility limit of hydrogen in solid iron, the hydrogen will be rejected during solidification, and this leads to pinhole formation and porosity in steel. Just a few parts increase per million of hydrogen dissolved in molten steel can cause hairline cracks (flakes), hydrogen embrittlement and loss of tensile ductility, particularly in large steel castings process. In practice, the hydrogen content of liquid steel is considerably less than the solid solubility limit. As a result, gross porosity in steel castings due to Hydrogen expulsion during solidification seldom occurs in practice. During cooling in the mold, however, a point may be reached when the steel becomes saturated with hydrogen and, on further cooling, is expelled from solution. This gas diffuses in an atomic form by lattice migration through the matrix. In other words, on transformation from γ (austenite) to α (ferrite), hydrogen becomes instantaneously less soluble but more easily diffusible. This is a major cause of the susceptibility of ferritic steels to hydrogen cracking and embrittlement, the matrix being easily supersaturated with highly mobile hydrogen. Microstructural features like grain boundaries, inclusion interfaces, pores, voids, etc., can act as effective traps (sinks) for hydrogen. In general, trapping effects become appreciable at temperatures below about 1500 C, the

atomic hydrogen being "desorbed" from the matrix to form molecular hydrogen. In fact, trapping effects are believed to be responsible for castings being less prone to hydrogen cracking and embrittlement than wrought. Products owing to the higher volume fraction of microstructural traps - these traps are "welded up" during thermomechanical processing high sulphur steels being less susceptible to hydrogen cracking and embrittlement by providing abundant inclusion interfaces for hydrogen recombination - a high volume fraction of non-planar inclusions is to be preferred [1-4].

When liquid steels cool from a temperature above austenitization temperature, it transforms into other phase configurations according to the austenite composition and cooling rate. As a result of phase transformation, the steel crystal structure and consequently, both the shape and the lattice parameter of the unit cell, change. These changes may introduce dilatational strains into the microstructure, which result in the creation of residual stress concentration zones within the microstructure. These stress concentration zones are vulnerable regions to the formation of micro cracks or growth of the flaws in these regions. Three processes are involved pertaining to hydrogen: (1) hydrogen evolution from the molten steel and segregation of hydrogen in casting part during solidification, (2) homogenization and redistribution of hydrogen in steel during solidification and (3) hydrogen diffusion from casting part during cooling. Hydrogen diffusion is considered paramount to obtain high-quality casting part with low hydrogen content. At or near room temperature, diffusible hydrogen is considered mobile, whereas residual hydrogen is trapped in the metal. Residual hydrogen can be retained through interaction with microstructural discontinuities or by the formation of hydrides with alloying elements. The presence of the factor of hydrogen leads to the formation of internal defects, such as capillary cracks, fracture cracks or lag. These defects begin to occur below 200 °C and generally continue throughout post-casting processes. It is very difficult to prevent hydrogen diffusion into the structure of liquid steel, except under vacuum processes. While there is no guarantee that hydrogen-containing steel will not fail due to hydrogen, 7 ppm of hydrogen is commonly considered the critical limit in foundries [5-7].

Hydrogen cracking occurs due to the buildup of gas pressure at inclusions, these are generally manganese sulfide inclusions. Mechanism for hydrogen cracking; Hydrogen is present in the steel as very small atoms. These small and active hydrogen atoms diffuse to energetically favorable sites i.e., surfaces which in the steel matrix are principally non-metallic inclusions. Hydrogen cracking is more likely to occur in segregated areas which contain hard phases. Hydrogen cracking is characterized by its fine, hairline stepped appearance linking inclusions [8-9].

Although the main task of the gating system is to direct the molten metal and fill the mold with molten metal, a well-designed gating system plays an important role in preventing various casting defects and metal turbulence in the casting process. Turbulence during the pouring of metals generates two main defects: (1) entrained air bubbles and (2) entrained oxide films from the surface of the liquid metal. The oxides are always entrained with the dry top surface of the oxide folded over against itself. This unbonded double interface (a bifilm) acts as a crack in the liquid metal, leading to the initiation of cracks and hot tears in the casting. All cracks and hot tears appear to be the product of entrained bifilms. The entrained air bubbles create a very serious surface area, increasing the probability of the hydrogen in the air bubbles to diffuse into the liquid steel [10-20]. This article aims to establish a relationship between the molding design and gating system design of steel casting parts produced by the sand mold casting method and hydrogen-induced defects.

In this study, the molding and gating system design of the part was changed to minimize turbulence of the liquid metal during mold filling. In this way, the interaction of the liquid steel with the air is minimized and the probability of snatching hydrogen from the humidity in the air was reduced.

2. Material and Method

In this study, it has been aimed to relate hydrogen induced cracks for steel castings by molding design and gating system design. The molding systems designs of the casting part are based on the modulus and geometry of the casting part. In the study, the material of the casting part is determined according to the SEW 520 standard and material of the casting part has been selected as G 14NiCrMo10-6. The part with two different molding designs and gating system designs have been molded in the flaskless resin molding system and casted in ÇİMSATAŞ foundry. The chemical composition of the casting part has been selected as shown in Table 1 and the image of the casting part is shown in Figure 1.

Table 1. Chemical composition of the casting part.

Contents (%)	C	Mn	S	Mo	P	Cr	Ni	Si	V	Cu	Al	Nb	Ti	Pb	Sn
Min.	0,12	0,55	0	0,45	0	1,3	2,7	0	0	0	0,02	0	0	0	0
Max.	0,16	0,70	0.010	0,55	0,010	1,8	3,0	0,30	0,003	0,35	0,08	0,06	0,05	0,02	0,03

In the first casting design study, gating system design of the casting part is based on total gross weight of the part (total gross weight including gating system and feeders) and effective casting height. Total gross weight of the casting part is 463 kg and effective casting height is 98 cm. The gating system ratio of the casting part has been chosen as 1:3:1. The gating system has been designed by using solid data and then, flow and solidification of the

casting part has been simulated at 1600°C by choosing lip pouring ladle. According to simulation results, designed gating system has been assembled to the casting part model. The designed gating system ratios and dimensions of the casting part are shown in Table 2 and the images of the simulation results of the casting part are shown in Figure 2.

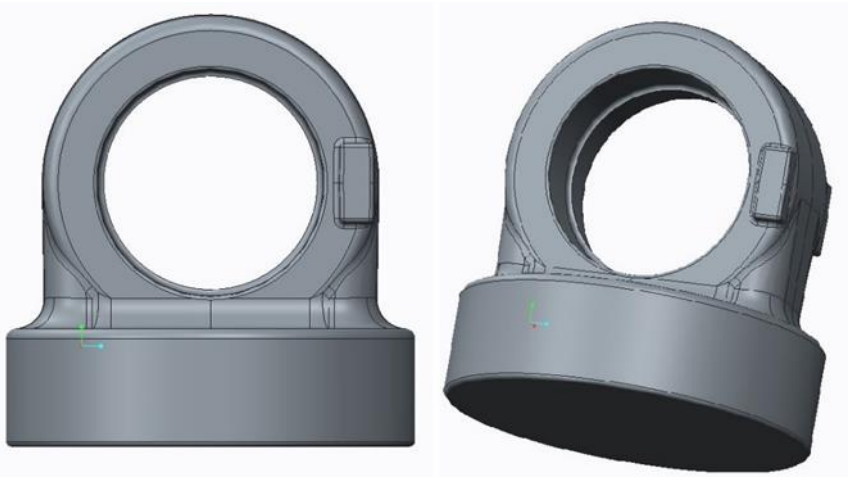

Figure 1. Schematic representation of the casting part.

Table 2. First designed gating system ratios and dimensions.

Gating system ratio	Vertical runner	Horizontal runner	Ingate
1:3:1	1	3	1
	16.37 cm^2	49.11 cm^2	16.37 cm^2

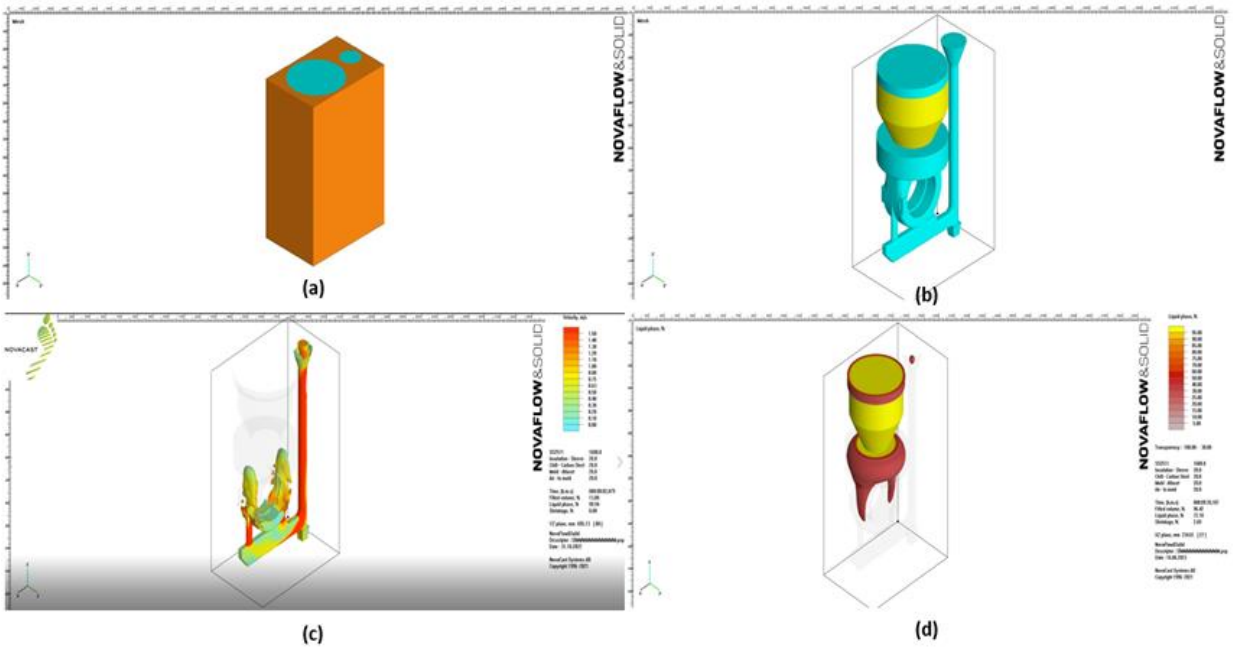

Figure 2. (a); The image of the molding design of the casting part, **(b);** The image of the casting part geometry, **(c);** The image of the metal flow and filling simulation of the casting part, **(d);** The image of the friction liquid mod of the casting part.

After simulation results, one part was molded in the flaskless resin molding system in ÇİMSATAŞ foundry. The Heraeus Hydris® was used to measure hydrogen levels in the liquid metal before and after casting. With this method, the increase in the amount of hydrogen experienced during the casting stage was detected. According to the measurements made on the part whose first gating system was designed, a hydrogen increase of 2.3 ppm was detected after 4 minutes of casting and waiting time in liquid steel with a hydrogen increase of 3.3 ppm during the 2 hour melting process. The fact that there is an increase that is almost equal to the increase in the entire melting process in just 4 minutes shows how important the casting stage is in terms of hydrogen level. After the hydrogen measurement of the liquid metal, the casting has been carried out with a lip pouring ladle at 1590 °C and in 30 seconds. Total gross weight of the casting part has been detected as 454 kg. The hydrogen measurement results of

the liquid metal are shown Figure 3 and The Image of the poured part with designed gating system is shown in Figure 4.

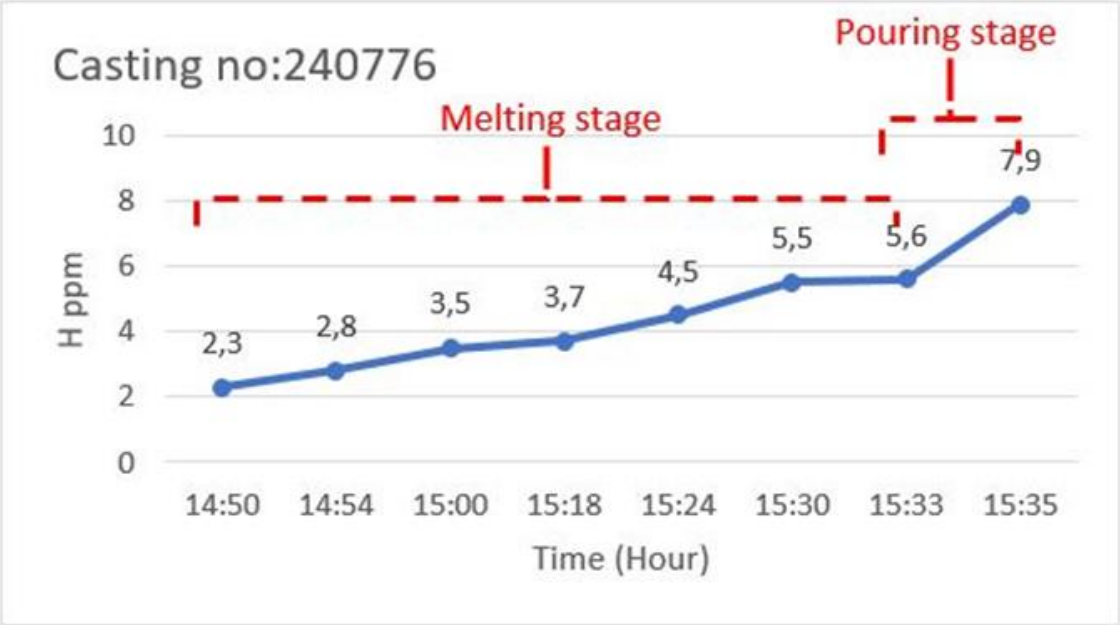

Figure 3. Hydrogen level measurement results during melting stage and pouring stage of the liquid metal.

Figure 4. The image of the poured casting part.

After the casted part was heat treatment (normalizing and tempering), the flange of the casting part was machined according to technical drawing of the part and magnetic particle testing was performed on the part. The locations of the defects and morphologies in the flange of the casting part under UV light after machining are shown in Figure 5.

Sample was taken from the defects area of the casting part after machining, and their examinations were carried out under Scanning Electron Microscopy (QUANTA FEG 250 SEM) and optical microscope (Zeiss Axio Vert A1) in the FOSECO Netherlands R&D center. The image of the sample taken from the defect area of the casting part under UV light is shown in Figure 6.

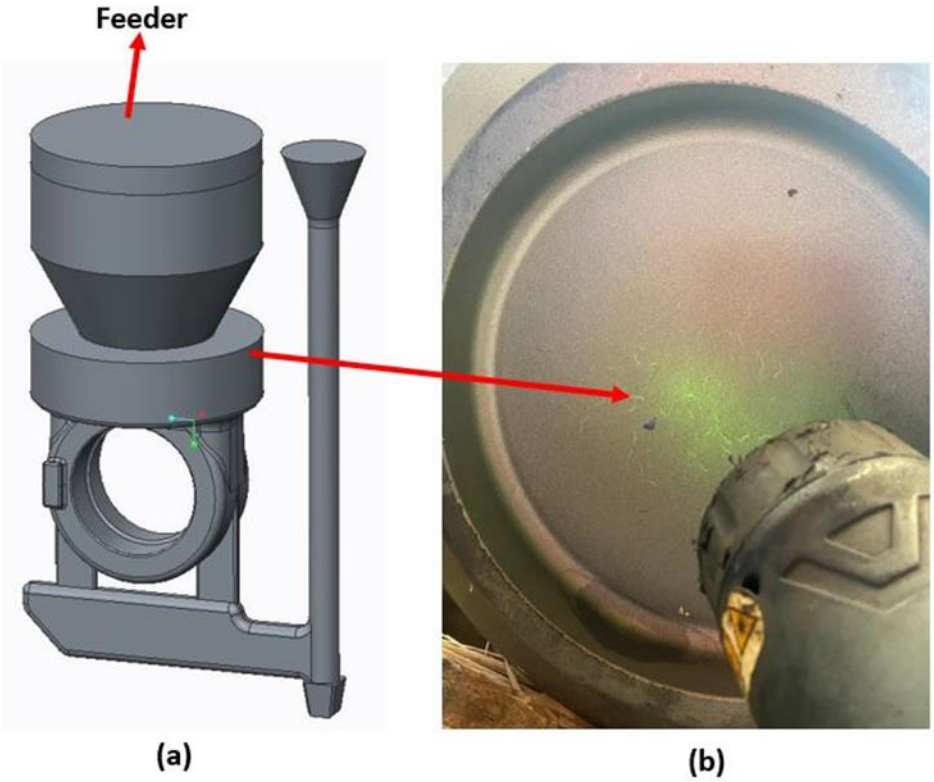

Figure 5. (a); The image of the molding design of the casting part, **(b);** The locations and morphologies of the defects on the flange of the casting part under UV light after machining.

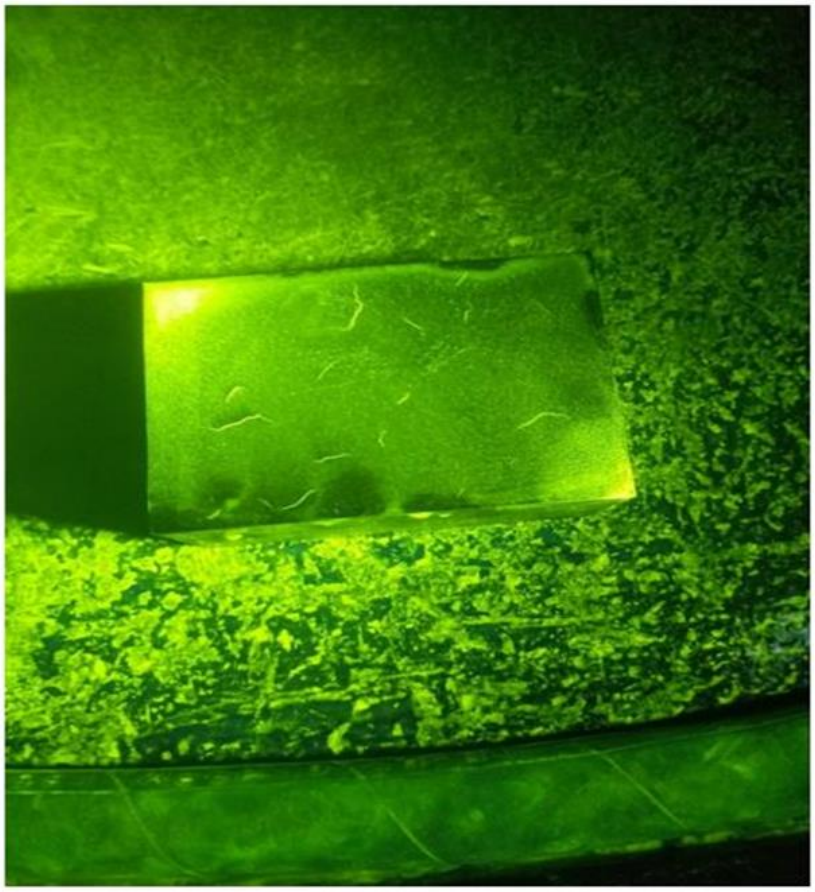

Figure 6. The image of the sample taken from defects area of the casting part.

The sample sent to FOSECO Netherlands R&D Center was cut with a saw and the crack depth in the sample was visually inspection. The original crack depth of the sample is shown in Figure 7.

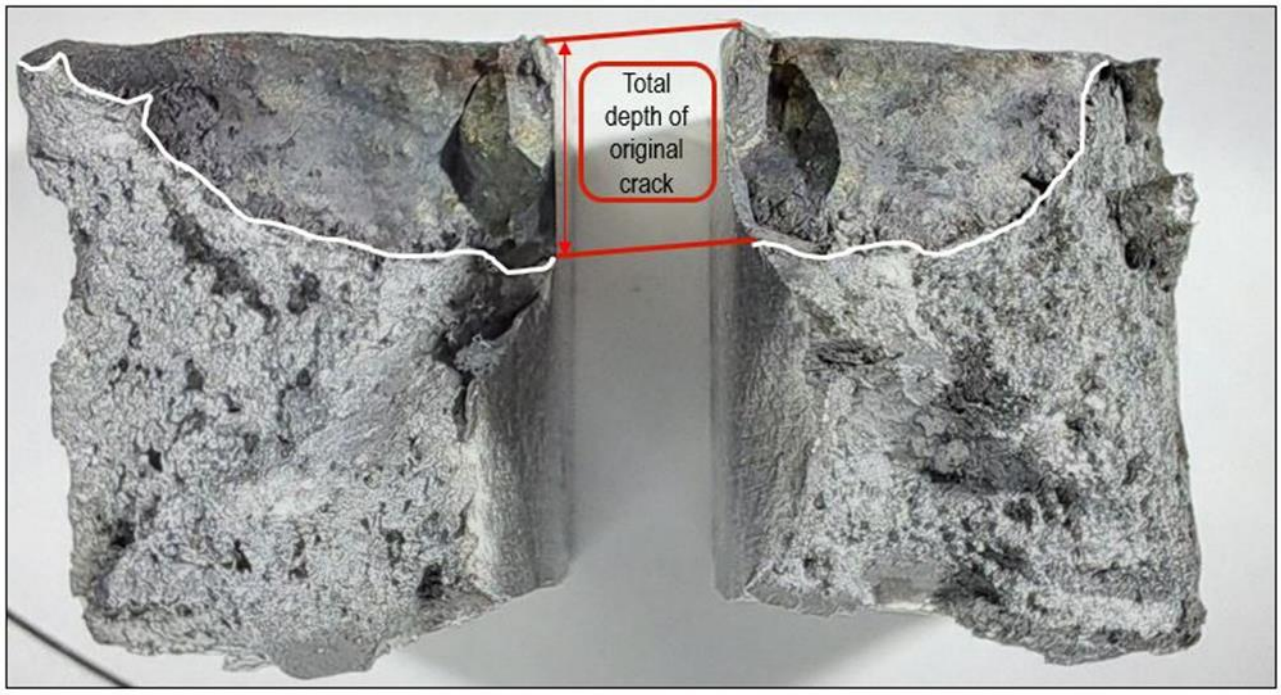

Figure 7. The image of the original crack depth of the sample.

Sample was examined from the cross section under the optical microscope un-etched condition. In the sample, which was examined under an optical microscope, it was observed that there were two areas of defects on the surface defect (1) and hidden crack below the surface (2). The images of sample under the optical microscope are shown in Figure 8 and Figure 9.

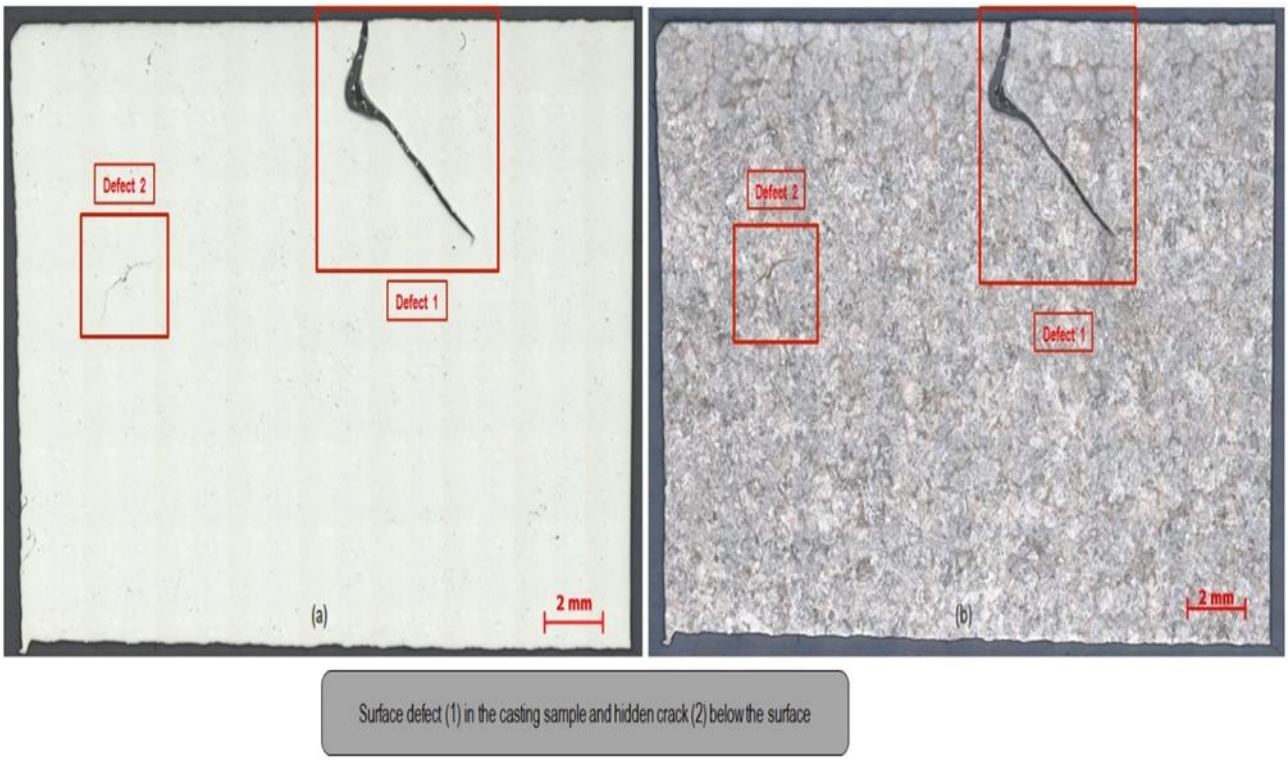

Figure 8. (a); The image of sample in the unetched condition under the optical microscope (5x), **(b);** The image of sample in the etched condition under optical microscope (5x).

After the defect 1 in sample was examined under the optical microscope, the defect 1 in the sample was examined with the Scanning Electron microscopy (SEM: 20 kV of accelerating voltage and 75x magnification) and EDX (energy dispersive X-ray analyzer). In the EDX analysis of defect 1, at the surface of the crack an iron oxide layer and in the defect some inclusions of Al and Si were detected. SEM micrographs and EDX analysis images of defect 1 are shown in Figure 10.

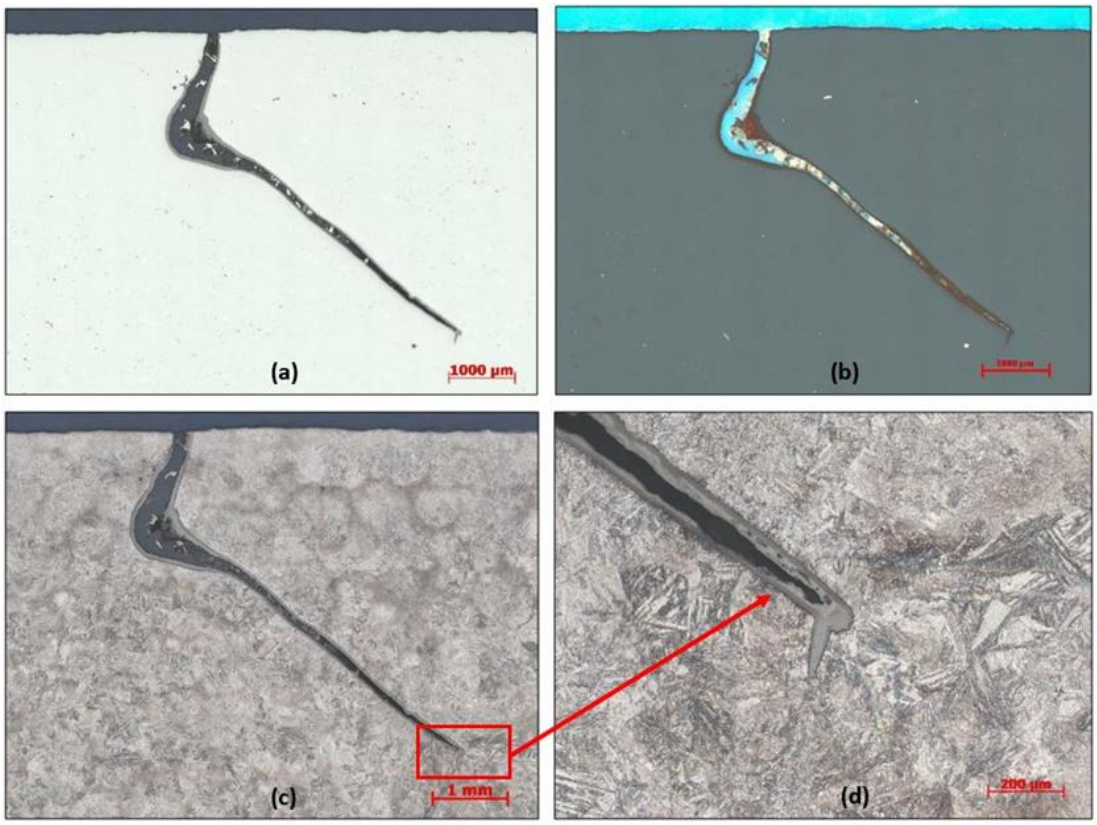

Figure 9. (a); Defect 1 unetched condition brightfield light (50x), **(b);** Defect 1 unetched condition polarized light (20x), **(c);** Defect 1 etched condition brightfield light (50x), **(d)**; Defect 1 etched condition brightfield light (100x).

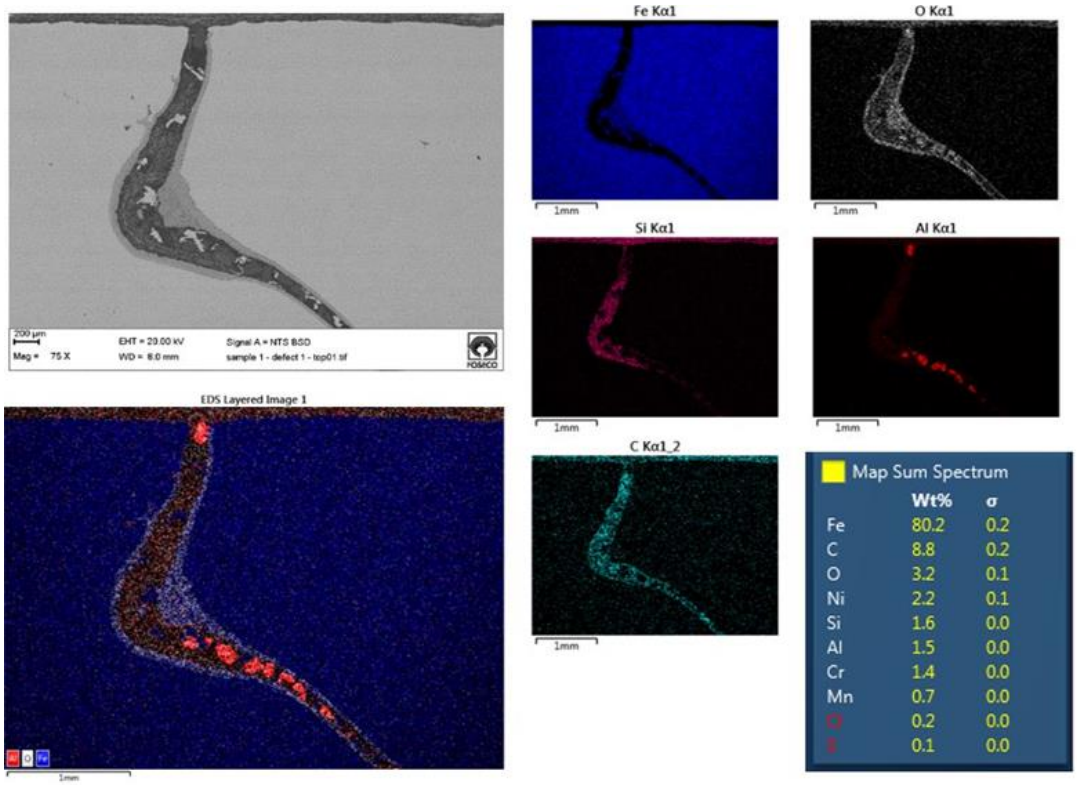

Figure 10. SEM micrographs (75x) and EDX analysis images of defect 1.

After the defect 1 in sample was examined with the SEM and EDX analysis, hidden crack below the surface (defect 2) in the sample was examined from the cross section under the optical microscope. When the defect 2 characteristic was examined under the optical microscope. The images of sample under the optical microscope are shown Figure 11.

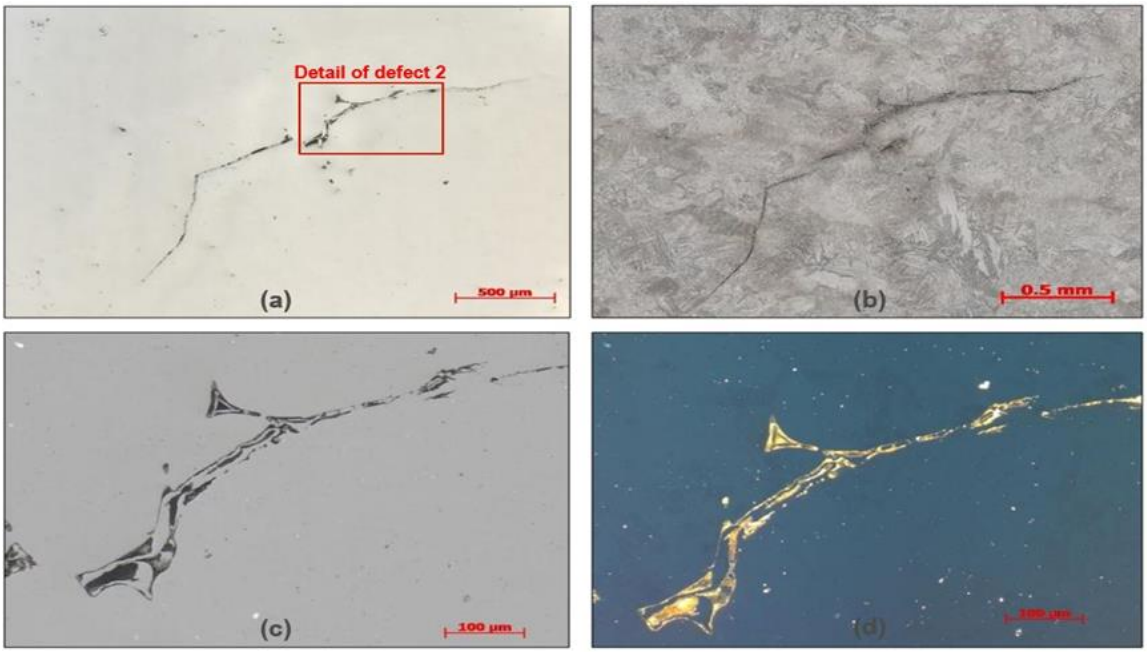

Figure 11. (a); Defect 2 unetched condition brightfield light(10x), **(b);** Defect 2 etched condition brightfield light (20x), **(c);** Defect 2 unetched condition brightfield light (100x), **(d)**; Defect 1 unetched condition polarized light (100x).

After the defect 2 in sample was examined under the optical microscope, the defect 2 in the sample was examined with the Scanning Electron microscopy (SEM: 20 kV of accelerating voltage and 400x-1500x magnification) and EDX (energy dispersive X-ray analyzer). In the EDX analysis of the defect 2, in the defect there is a higher amount of Al and O detected. Moreover, in the defect some inclusions of S, Mn and Si are detected (e.g., MnS). SEM micrographs and EDX analysis images of defect 2 are shown in Figure 12 and Figure 13.

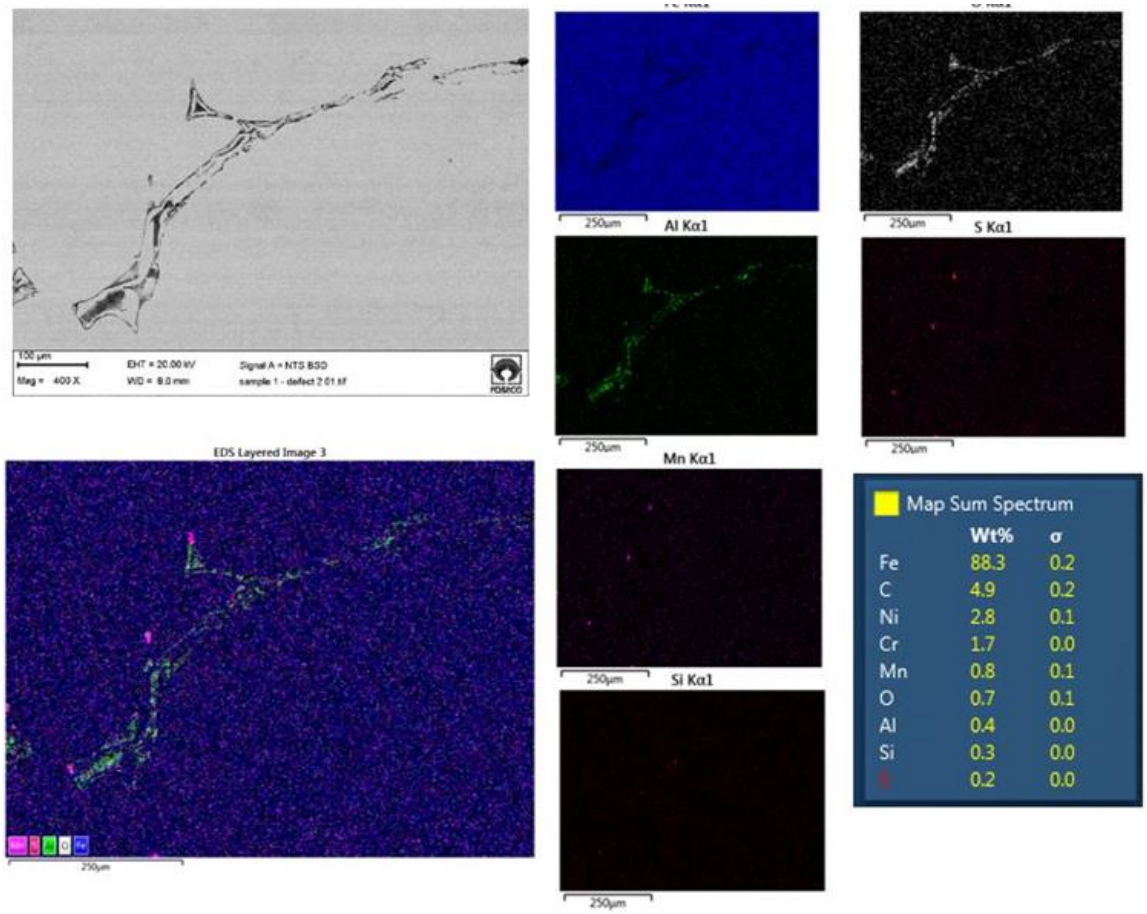

Figure 12. SEM micrographs (400x) and EDX analysis images of defect 2.

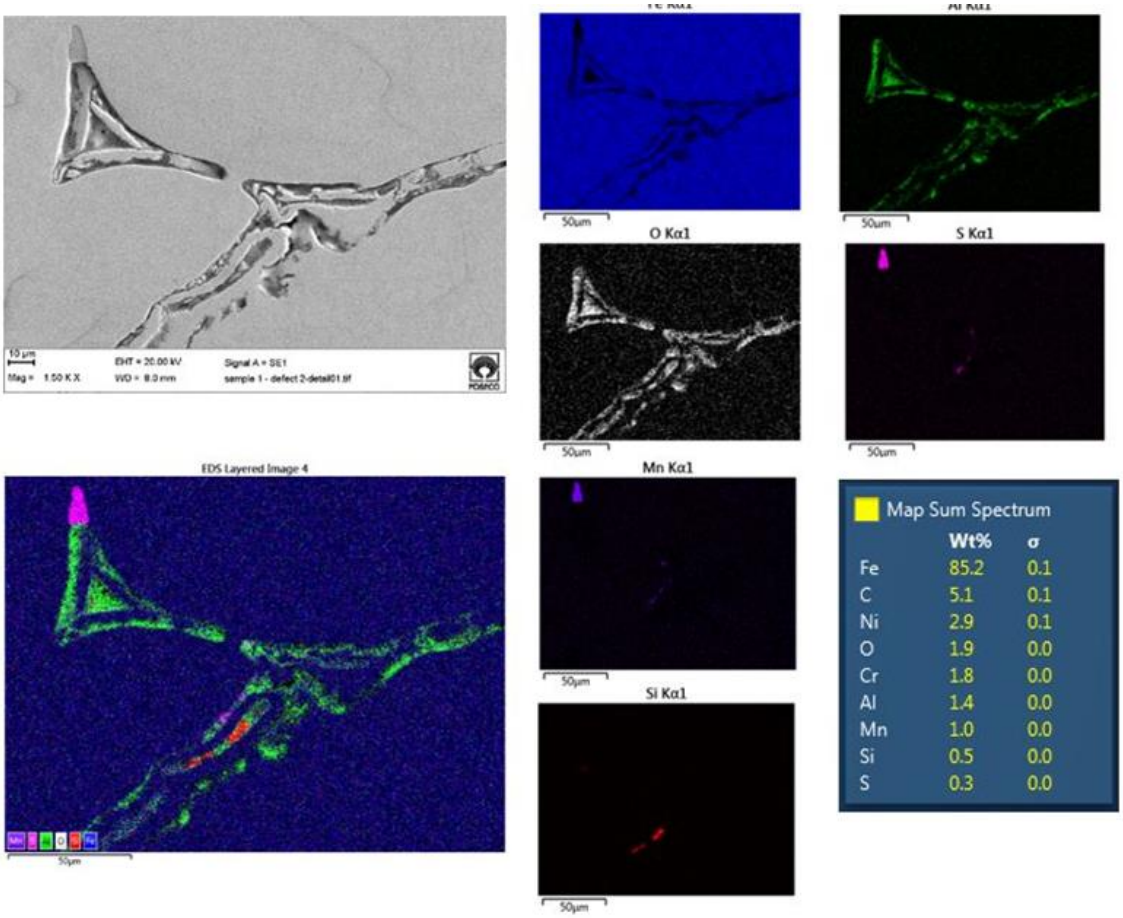

Figure 13. SEM micrographs (1500x) and EDX analysis images of defect 2.

After the defect 2 in sample was examined with the SEM and EDX analysis, was used by the metal extraction method to determine the hydrogen and nitrogen content of the sample. To determine the hydrogen and nitrogen content, 4 samples of approximately 1 gram each were taken from the sample. The measurements were carried out by the method of melting extraction according to the accredited process instruction VA7-13:2016-10(*).

Determination of hydrogen content measurement procedure was calibrated with pure hydrogen and rechecked with a reference standard of 2.5 ±0.2 ppm. The values of the calibration measurement were in this range. A recalibration was not necessary during the entire measurement. The detection limit of this measuring method is 0.3 ppm. The results of the hydrogen content of the sample are shown in Table 3.

Table 3. Results of the determination of the hydrogen content.

Component	Method of measurement	Content of hydrogen (ppm)		Average (ppm)
		1.Measurement	2.Measurement	
Steel cast sample	Melting extraction	0.4	0.4	0.4

After the hydrogen content of the sample was determined, the nitrogen content of the sample was determined by the metal extraction method. Determination of hydrogen content measurement procedure was calibrated with pure hydrogen and rechecked with a reference standard of 69 ±3 ppm. The values of the calibration measurement were in this range. The results of the hydrogen content of the sample are shown in Table 4.

Table 4. Results of the determination of the nitrogen content.

Component	Method of measurement	Content of hydrogen (ppm)		Average (ppm)
		1.Measurement	2.Measurement	
Steel cast sample	Melting extraction	66	73	69.5

After the first poured part was examined and then molding and gating system design of the casting part was changed in the part solid data. In the casting part design, the gating system design of the casting part was calculated according to total gross weight and effective casting height of the part. Total gross weight of the casting part is 500 kg and effective casting height of the casting part is 32 cm. After the gating system design of the casting part was chanced, flow and solidification of the part was simulated at 1600 °C by choosing lip pouring ladle. According to simulation results of the part, the gating system was assembled to the casting part model. The designed gating

system ratios and dimensions of the casting part are shown in Table 5 and the images of the simulation results of the casting part are shown in Figure 14.

Table 5. Second designed gating system ratios and dimensions.

Gating system ratio	Vertical runner	Horizontal runner	Ingate
1:3:1	1	3	1
	17,26 cm²	51,78 cm²	17,26 cm²

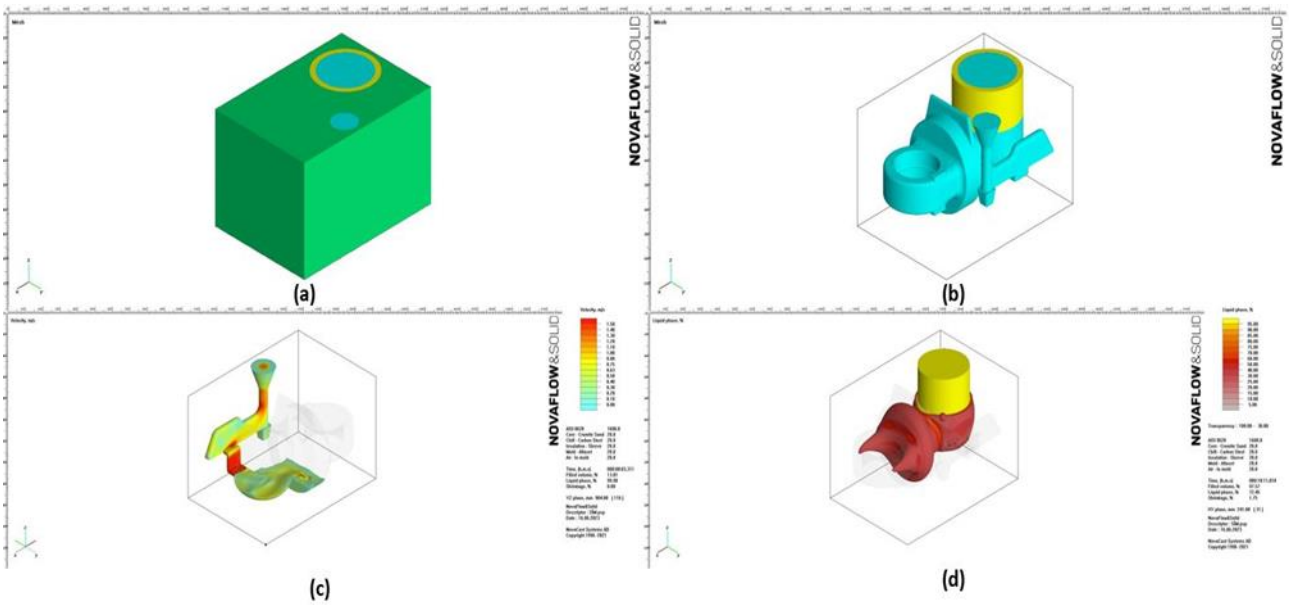

Figure 14. (a); The image of the molding design of the casting part, **(b);** The image of the casting part geometry, **(c);** The image of the metal flow and filling simulation of the casting part, **(d);** The image of the friction liquid mod of the casting part.

After simulation results, one part was molded again in the flaskless resin molding system in ÇİMSATAŞ foundry. Before and after the casting process, hydrogen measurements of the liquid metal by Heraeus Hydris® hydrogen measuring device was used. According to the measurements made on the part whose second casting part was designed, obtained measurement results were compared with the first measurements. As can be seen in Figure 15, while hydrogen level of the liquid metal is 6.4 ppm before pouring stage, it is 7 ppm after the pouring stage. Hydrogen increase is only 0.6 ppm in second designed casting part. Hydrogen increase was 2.3 ppm (in the pouring stage) in the previous design of the casting part. After the hydrogen measurement of the liquid metal, the casting has been carried out with a lip pouring ladle at 1590 °C and in 35 seconds and total gross weight of the casting part has been detected as 492 kg. The Image of the new designed casting part is shown in Figure 16.

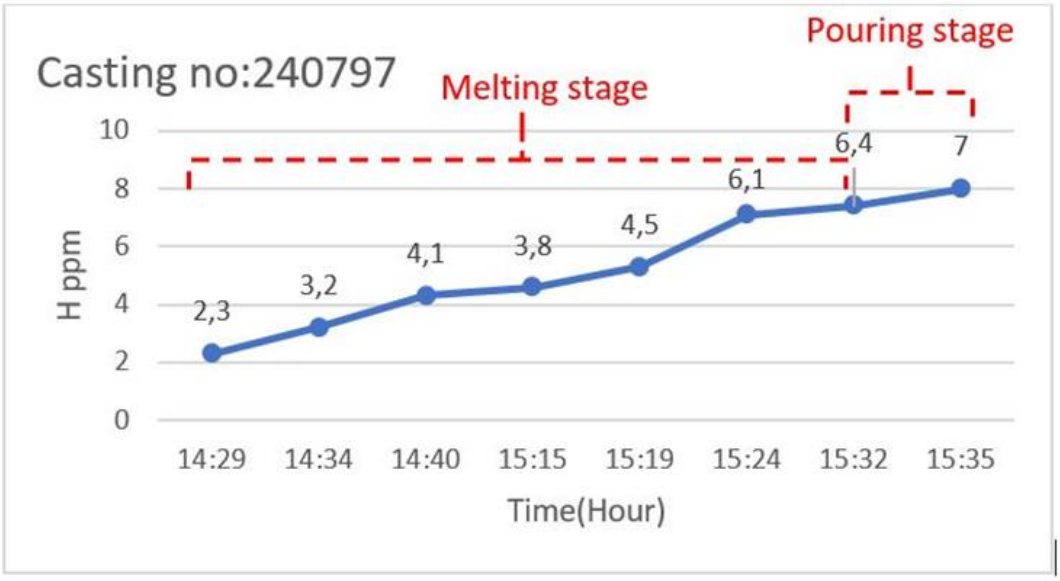

Figure 15. Hydrogen level measurement results during melting stage and pouring stage of the liquid metal.

Figure 16. The Image of the new designed casting part**.**

After the casted part with new designed was heat treatment (normalizing and tempering), the flange of the casting part was machined according to technical drawing of the part and magnetic particle testing was performed on the part. It was observed that there were no defects under UV light in the magnetic particle test applied to the flange of the cast part after machining. The flange of the casting part under UV light after machining are shown in Figure 17.

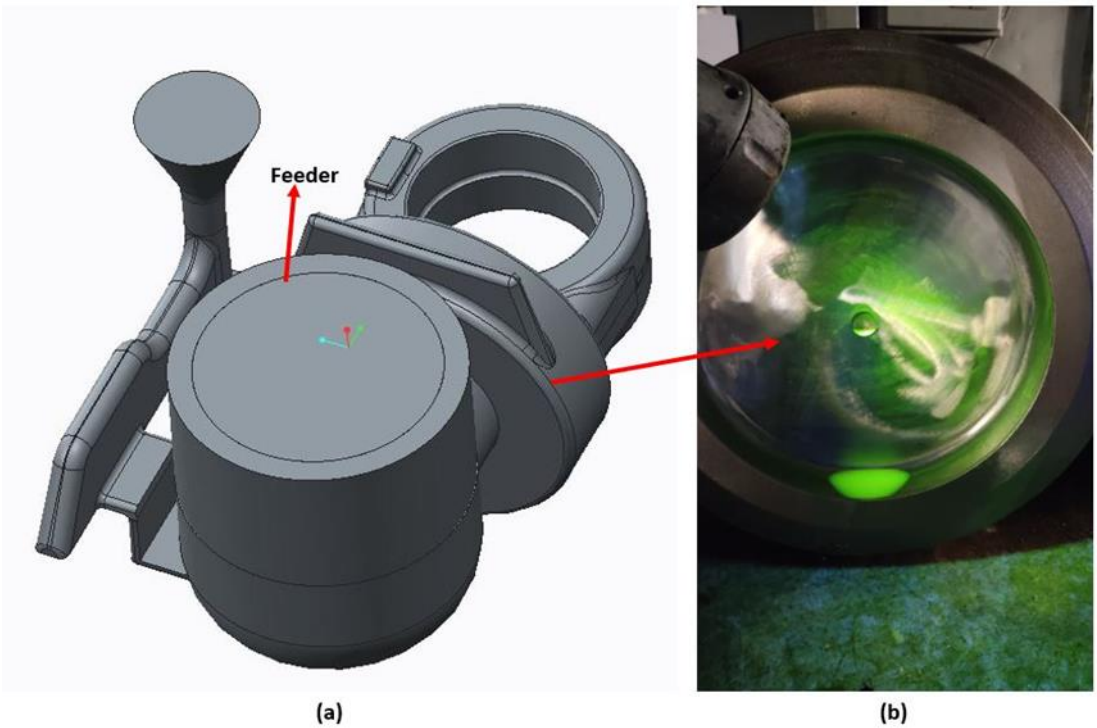

Figure 17. (a); Image of the mold design of the cast part, **(b);** Image of the flange of the casting part under UV light after machining.

3. Results

In this article, the casting parts have been designed according to the simulation results with different molding and gating system designs by using the material G 14NiCrMo10-6 steel castings. The findings were obtained from the simulations results, optical microscope inspections, SEM - EDX analyzers and poured parts.

- It was found that the simulation results cannot detected hydrogen induced defects in the casting part.
- While it was observed that turbulence occurred in the liquid metal in the filling simulation of the first designed casting part, it was observed that there was no turbulence in the liquid metal in the filling simulation of the second casting part designed.
- It was observed that the total gross weight of the first designed casting part was 454 kg, the total gross weight of the second designed casting part was 492 kg.
- While the filling time of the poured part with the first designed casting part was 30 seconds, the filling time of the poured part with second designed was increased to 35 seconds.
- The observed crack-like defects very probably run along the former primary grain boundaries of the cast steel.
- They are therefore more likely to have arisen before the normalization annealing.
- Some cracks must have had a connection to the surface during normalization, as their surface is heavily oxidized (layer of scale).
- The structure of the steel shows a relatively large number of non-metallic inclusions (Al oxide, MnS), also in the vicinity of the crack-like defects. Such inclusions have a strength-reducing effect and are also traps for hydrogen.
- All inclusions that could be found within the cracks very likely got there later (during processing, handling).
- The cracks are predominantly relatively wide open, which is atypical for cracks caused exclusively by mechanical stresses (near room temperature). The effect of stresses during quenching of the casting can be ruled out because the cracks were already detected before hardening.
- In Heraeus Hydris® hydrogen measurements, it was observed that the hydrogen level of the liquid metal in both casting designs was less than the critical value of 8 ppm.
- The hydrogen and nitrogen levels found in a sample (by metal extraction method) are not critical (0.4 and 69.5 ppm respectively). Despite the low H content, hydrogen is probably the cause of this cracking.
- The source of the hydrogen cannot be determined afterwards. During solidification, the hydrogen dissolved in the melt segregated into the areas that solidified last and then led to the cracking of the primary grain boundaries (called as flakes in the steel industry).
- During the subsequent heat treatment (tempering), the hydrogen was expelled from the material so that it could no longer be detected later.

4. Conclusion

The study aimed to establish a relationship between hydrogen-induced defects in steel castings and the design of both molding and gating systems. The findings of this investigation have shed light on the connection between these defects and the design aspects of the molding and gating systems. Notably, the study revealed that hydrogen-induced crack defects were particularly associated with NiCr, NiCrMo, and NiCrMoV steel materials.

One key factor contributing to these defects is the turbulence experienced by the liquid metal during the casting process. This turbulence leads to the formation of re-oxidation products within the alloying elements present in the liquid metal. Moreover, this turbulent flow in the liquid metal significantly increases the contact between the metal and any free moisture present in the mold during the casting process. As a result, this heightened interaction is found to be a major cause of the hydrogen-induced defects observed in the resulting steel castings. These findings underscore the importance of carefully considering both molding and gating system design to mitigate the occurrence of hydrogen-induced defects in steel castings, especially when utilizing sensitive steel materials like NiCr, NiCrMo, and NiCrMoV.

Acknowledgement

We would like to thank ÇİMSATAŞ General Manager Mr. Fatih Erdoğan, ÇİMSATAŞ Production Group Manager Mr. Necmettin Acar, ÇİMSATAŞ Foundry Manager Mr. Kazım Çakır, ÇİMSATAŞ Foundry Production Chief Mr. Buğra Erbakan, ÇİMSATAŞ Production Engineer Mr. Vedat Uz, ÇİMSATAŞ Foundry Finishing Engineer Mr. Mert Demirdöğen, FOSECO Netherlands R&D Center Manager Mr. Derya Dispinar, FOSECO Netherlands R&D Int. Tech. Manager Mr. Wolfram Stets, FOSECO Netherlands R&D Analytical Lab. Specialist Mr. Edwin Onland.

This study was partly presented in the 7th Advanced Engineering Days (AED) [21].

Funding

This research received no external funding.

Author contributions

Mustafa Murat Zor: Conceptualization, Methodology, Design, Simulation, Writing-Original draft preparation, Editing, , **Ferhat Tülüce:** Validation, Editing, **Serdar Kesim:** Validation, **Alper Yoloğlu:** Editing

Conflicts of interest

The authors declare no conflicts of interest.

References

1. Xian, A., Li, P., Chen, W., Wang, Y., Chen, R., & Mei, D. (1994). Effect of removing hydrogen from heavy rail steel blooms by stack cooling in Panzhihua iron and steel company. Acta Metallurgica Sinica, Series A, 6, 415-419.
2. Fruehan, R. J. (1997). A review of hydrogen flaking and its prevention. Iron & steelmaker, 24(8), 61-69.
3. Bramfitt, B. L. (2005). Carbon and Alloy Steels. Mechanical Engineers' Handbook: Materials and Mechanical Design, 1, 1-38.
4. Akhurst, K. N., & Baker, T. J. (1981). The threshold stress intensity for hydrogen-induced crack growth. Metallurgical Transactions A, 12, 1059-1070. https://doi.org/10.1007/BF02643487
5. Archakov, Y. I., & Grebeshkova, I. D. (1986). Nature of hydrogen embrittlement of steel. Metal Science and Heat Treatment (Engl. Transl.); (United States), 27.
6. Bugaev, V. N., Gavriljuk, V. G., Petrov, Y. N., & Tarasenko, A. V. (1997). Mechanism of hydrogen-induced phase transformations in metals and alloys. International journal of hydrogen energy, 22(2-3), 213-218. https://doi.org/10.1016/S0360-3199(96)00154-1
7. Barrera, O., Tarleton, E., Tang, H. W., & Cocks, A. C. F. (2016). Modelling the coupling between hydrogen diffusion and the mechanical behaviour of metals. Computational Materials Science, 122, 219-228. https://doi.org/10.1016/j.commatsci.2016.05.030
8. Ravichandar, D., Balusamy, T., & Nagashanmugam, K. B. (2014). Reducing UT rejections in Cr-Mo and High Mn steels by controlling hydrogen and optimising superheat. Applied Mechanics and Materials, 591, 38-42. https://doi.org/10.4028/www.scientific.net/AMM.591.38
9. Gaude-Fugarolas, D. (2010). Hydrogen reduction during steel casting by thermally induced up-hill diffusion. Proceedings of METAL2010, Roznov pod Radhostem, Czech Republic. Tanger Ltd.
10. Campbell, J. (2015). Complete casting handbook: metal casting processes, metallurgy, techniques and design. Butterworth-Heinemann.
11. Zor, M. M., Yoloğlu, A., Kesim, S., & Tülüce, F. (2022). Pressurized gating system design and optimization in steel castings. Engineering Applications, 1(1), 1-10.
12. Jolly, M. (2005). Prof. John Campbell's ten rules for making reliable castings. Jom, 57, 19-28.
13. Campbell, J. (2012). Stop pouring, start casting. International Journal of Metalcasting, 6, 7-18. https://doi.org/10.1007/BF03355529
14. Melendez, A. J., Carlson, K. D., & Beckermann, C. (2010). Modelling of reoxidation inclusion formation in steel sand casting. International Journal of Cast Metals Research, 23(5), 278-288. https://doi.org/10.1179/136404610X12693537269976
15. Renukananda, K. H., & Ravi, B. (2016). Multi-gate systems in casting process: comparative study of liquid metal and water flow. Materials and Manufacturing Processes, 31(8), 1091-1101. https://doi.org/10.1080/10426914.2015.1037911
16. Brown, J. (2000). Foseco ferrous foundryman's handbook. Butterworth-Heinemann. 11th ed., Butterworth-Heinemann, Oxford.
17. Zor, M. M., Kesim, S., Tülüce, F., & Yoloğlu, A. (2023). Reducing casting defects in ductile iron castings by optimized pouring system. Engineering Applications, 2(1), 26-31.
18. Modaresi, A., Safikhani, A., Noohi, A. M. S., Hamidnezhad, N., & Maki, S. M. (2017). Gating system design and simulation of gray iron casting to eliminate oxide layers caused by turbulence. International Journal of Metalcasting, 11(2), 328-339. https://doi.org/10.1007/s40962-016-0061-3
19. Hsu, F. Y., Jolly, M. R., & Campbell, J. (2009). A multiple-gate runner system for gravity casting. Journal of Materials Processing Technology, 209(17), 5736-5750. https://doi.org/10.1016/j.jmatprotec.2009.06.003

20. Jezierski, J. D. R. & Jenerka, K. (2017). Optimizing Gating System for Steel Castings. In 5th International Conference on Modern Manufacturing Technologies in Industrial Engineering, 14-17.
21. Zor, M. M., Tülüce, F., Kesim, S., & Yoloğlu, A. (2023). The effect of metal turbulence on hydrogen induced crack defects in steel castings. Advanced Engineering Days (AED), 7, 92-95.